Mathematical Modelling of Engineering Problems
Vol. 12, No. 3, March, 2025, pp. 999-1006
Journal homepage: http://iieta.org/journals/mmep

Backstepping Sliding Mode Control for Magnetic Levitation Position Control: Design and Analysis

Ahmed Khalaf Hamoudi, Luay Thamir Rasheed*

Control and Systems Engineering Department, University of Technology-Iraq, Baghdad 10066, Iraq

Corresponding Author Email: luay.t.rasheed@uotechnology.edu.iq

https://doi.org/10.18280/mmep.120326

Received: 20 March 2024
Revised: 19 June 2024
Accepted: 28 June 2024
Available online: 31 March 2025

Keywords:
Maglev, CSMC, BSC, MSMC, BSSMC

ABSTRACT

The aim of this study is to improve the performance of the sliding mode controller (SMC) for controlling and stabilizing a steel ball of the Magnetic Levitation (Maglev) system at a desired position with the existence of disturbance, noise and parameters uncertainty in the system model. This enhancement is achieved by replacing the equivalent control law of the SMC with the backstepping control law to construct a controller from the backstepping controller (BSC) and the SMC to have a new controller called the backstepping sliding mode controller (BSSMC). Due to the nonlinearity of the system model, nonlinear and robust controllers such as BSSMC have been designed. The suggested controller can successfully reduce the settling time, which is regarded as an essential property in control system engineering. The simulation results obtained using the MATLAB program demonstrated the proposed controller's effectiveness. The comparison of results between the BSSMC and other controllers indicated a smaller settling time in BSSMC. The Lyapunov theory has been adopted to check the system's stability when applying the BSSMC controller.

1. INTRODUCTION

The Maglev system has many applications because it eliminates energy losses caused by surface friction. The Maglev system is a technique that allows an object (the ball) to float in the air without support. Therefore, it must generate a flux by controlling the amount of a coil current. The generated magnetic flux will be utilized to make the body levitate in the air at a predetermined distance from the coil position so that the body movement within that generated magnetic flux can be negligible [1]. The magnetic field's power is in the opposite direction to the gravity attraction of the ball, so the body will be lifted toward the coil. Using vibration isolation, this system is capable of solving the friction problem. Consequently, friction loss can be negligible in this system, which undoubtedly impacts both the desired response and the performance of the system [2].

The non-contact property with zero friction of the Maglev system makes it very popular, and it is considered as the future technology. The Maglev system has many applications, such as high-speed transportation systems, launching rockets, as well as other applications, etc. [3, 4]. Many controllers have been proposed to control the Maglev model, as discussed below.

Jose and Mija [5] proposed a fractional order sliding mode controller (FOSMC) for controlling the position of the Maglev system. The Particle Swarm Optimization (PSO) algorithm is employed to determine the fractional order switching surface and the order of the fractional derivative. Adil et al. [6] used supertwisting SMC and integral backstepping SMC for controlling the position of the Maglev model. The supertwisting SMC provides a superior dynamic response with negligible chattering and is robust against external disturbances in controlling the Maglev model compared to the integral backstepping SMC and other nonlinear controllers. Burakov [7] utilized a fuzzy PID controller for the Maglev system control system. The controller is structured with three channels, each with its own control function that characterizes the variation in the gain factor based on the input variable's value. The process of setting the controller entails performing genetic optimization algorithm in off-line mode. Wei et al. [8] used a deep neural network feedforward compensation controller based on an enhanced Adagrad optimization algorithm for the position control of the Maglev system. The control structure of the controller comprises a deep neural network identifier, a deep neural network feedforward compensator, and a PID controller. The performance proposed controller demonstrates good dynamic and static performance as well as some robustness. Humaidi et al. [9] proposed the design and analysis of the Active Disturbance Rejection Control (ADRC) approach for the control and disturbance rejection of the Maglev system. Two controllers are considered using the ADRC structure. These controllers are known as the Linear ADRC (LADRC) and Nonlinear ADRC (NADRC). A comparison of the robustness against parameter variation and the capability to reject applied disturbance of LADRC and NADRC has been conducted. The MATLAB simulation results showed that LADRC exhibits better robustness characteristics compared to NADRC. Moreover, when a specific disturbing force is applied to the ball mass, the

LADRC shows superior disturbance rejection capabilities compared to the NADRC.

MohammadRidha and Kadhim [10] used an Adaptive Variable Structure Controller based on barrier function (AVSCbf) for position control of the Maglev system. The performance of the AVSCbf has been compared with that of the Adaptive Variable Structure Controller without the barrier (AVSC) and the classical Variable Structure Controller (VSC). The simulation results show that the AVSCbf outperforms the AVSC and VSC in reducing steady-state error and improving disturbance rejection. Yadav et al. [11] utilized an optimized proportional-integral-derivative (PID) controller for position control of the Maglev system. The variables of the PID controller are optimized using Grey Wolf Optimizer (GWO). The proposed controller's effectiveness has been validated through comparison with a classical PID controller tuned using Ziegler-Nichols tuning criteria.

The following points summarize the contributions of this study:

• To enhance and develop the performance of the SMC for controlling the position of the steel ball of the Maglev model by replacing the equivalent control law of the SMC with the backstepping control law.

• To employ a BSSMC in order to better cope with the effect of the external disturbances that affect the position control of the Maglev system.

• To perform a comparative study of the controlled system performance utilizing a BSSMC and other controllers. The assessment of each controller used to control the position of the ball of the Maglev system is conducted based on minimizing the settling time and the external disturbance effect.

This work is addressed as follows: the mathematical model for the Maglev system is presented in section two. The controllers design for the SMC and BSSMC are explained in section three. In section four, the computer simulation results are discussed to verify the proposed controller's effectiveness. Finally, the conclusion is addressed in section five.

2. DESCRIPTION OF THE MATHEMATICAL MODEL

The position of the ball of the Maglev model is controlled by adjusting the coil current and, consequently, controlling the magnetic field produced by the coil, as shown in Figure 1. The applied voltage $u(t)$ can be described using Kirchhoff's voltage law, as follows [12, 13]:

$$u(t) = R\, i(t) + L\frac{di}{dt} \tag{1}$$

where, R represents the coil resistor, L represents the coil inductance, and $i(t)$ represents the current flowing in the coil. For $R >> L$, the Eq. (1) can be written as follows:

$$i(t) = k_1 u(t) \tag{2}$$

where, k_1 is the control voltage to coil current gain.

The equation for the motion of the steel ball influenced by gravity can be derived using Newton's principle of motion [13, 14]:

$$m\ddot{x}(t) = mg - f(x,i) + d(t) \tag{3}$$

where, m represents the mass of the ball, x represents the position of the ball, g represents the acceleration due to gravity, $f(x,i)$ represents the magnetic force, and d represents the disturbance.

A force that is generated as a result of the magnetic effect can be expressed as:

$$f(x,i) = \frac{i^2(t)}{2} L_o x_o \frac{1}{x^2(t)} \tag{4}$$

where, $i(t)$ represents the current flowing through the coil, L_o represents the increment in inductance due to the ball, x_o represents the equilibrium position of the levitating ball, and x represents the actual position of the levitating ball.

The equation of motion can be expressed as follows:

$$m\ddot{x}(t) = mg - k_o \frac{i^2(t)}{x^2(t)} + d(t) \tag{5}$$

$$k_o = \frac{L_o x_o}{2} \tag{6}$$

Finally, the equation of motion of the Maglev system can be expressed using Eqs. (2), (5), and (6) in the state space representation form as follows:

$$\dot{x}_1(t) = x_2(t) \tag{7}$$

$$\dot{x}_2(t) = g - \frac{k_o k_1^2}{m}\frac{u^2(t)}{x_1^2(t)} + d(t) \tag{8}$$

where, $u(t)$ represents the voltage control input to the Maglev system, $x_1(t)$ represents the steel ball position, and $x_2(t)$ represents the steel ball velocity.

The nominal parameters of the Maglev model are as presented in Table 1 [13, 14].

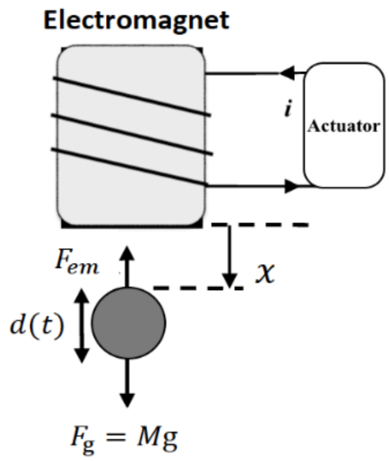

Figure 1. The schematic representation of Maglev model

Table 1. The physical parameters of the Maglev model [13, 14]

Parameters	Value	Unit
Mass of the ball (m)	0.02	kg
Acceleration due to gravity (g)	9.81	m/s^2
Control input voltage level (u)	±5	V
Equilibrium value of position (x_o)	0.009	m
Equilibrium value of current (i_o)	0.8	A
The increment in inductance due to ball (L_o)	5.518125×10^{-3}	H
Control voltage to coil current gain (k_1)	1.05	A/V

3. THE CONTROLLER DESIGN

The first design step involves defining the error $z_1(t)$ between the actual position of the ball $x_1(t)$ and the desired position $x_d(t)$ as follows [15-18]:

$$z_1(t) = x_1(t) - x_d(t) \tag{9}$$

The first- and second-time derivative of Eq. (9) can be obtained as follows:

$$\dot{z}_1(t) = \dot{x}_1(t) - \dot{x}_d(t) \tag{10}$$

$$\dot{z}_1(t) = x_2(t) - \dot{x}_d(t) \tag{11}$$

$$\ddot{z}_1(t) = \dot{x}_2(t) - \ddot{x}_d(t) \tag{12}$$

where, $x_1(t)$ is the actual position of the ball, $x_d(t)$ represents the desired position of the ball, and $x_2(t)$ is the actual velocity of the ball.

Eq. (12) can be expressed as follows:

$$\ddot{z}_1(t) = g - \frac{k_o k_1^2}{m}\frac{u^2(t)}{x_1^2(t)} + d(t) - \ddot{x}_d(t) \tag{13}$$

To design a SMC, the sliding surface can be expressed using the error equations provided in Eqs. (9) and (11) as follows:

$$s(t) = \lambda\, z_1(t) + \dot{z}_1(t) \tag{14}$$

where, λ is a positive constant.

The first-time derivative of the equation for a sliding surface is given by:

$$\dot{s}(t) = \lambda\left(x_2(t) - \dot{x}_d(t)\right) + g - \frac{k_o k_1^2}{m}\frac{u^2(t)}{x_1^2(t)} + d(t) - \ddot{x}_d(t) \tag{15}$$

By setting $(i = u)$, the above equation is written as follows:

$$\dot{s}(t) = \lambda\,(x_2(t) - \dot{x}_d(t)) + g - \frac{k_o k_1^2}{m}\frac{u^2(t)}{x_1^2(t)} + d(t) - \ddot{x}_d(t) \tag{16}$$

Based on SMC theory, the control law u consists of the following:

$$u_1 = u_{eq} + u_{sw} \tag{17}$$

where, u_{eq} represents the equivalent control law, and u_{sw} represents the switching control law.

These two control laws can be described as follows:

$$u_{eq} = \sqrt{\left(\frac{m x_1^2}{k_o k_1^2}\right)(\lambda x_2(t) - \lambda \dot{x}_d(t) + g - \ddot{x}_d(t))} \tag{18}$$

$$u_{sw} = K sat(s) \tag{19}$$

where, K represents a scaler design constant and $sat(s)$ represents the saturation function (boundary layer function) used instead of the signum function in the sliding mode control effort to avoid the chattering effect.

The saturation function is defined in Eq. (20) as follows:

$$sat(s) = \begin{cases} 1 & s \geq \Delta \\ \frac{s}{\Delta} & -\Delta < s < \Delta \\ -1 & s \leq -\Delta \end{cases} \tag{20}$$

where, Δ represents the boundary layer thickness.

When the sliding surface and its derivative are set to zero, the sliding mode control effort can be expressed as follows:

$$u_1 = \sqrt{\left(\frac{m x_1^2}{k_o k_1^2}\right)(\lambda x_2(t) - \lambda \dot{x}_d(t) + g - \ddot{x}_d(t) + K sat(s))} \tag{21}$$

The controlled system block diagram using MSMC for controlling the ball position of the Maglev model is shown in Figure 2.

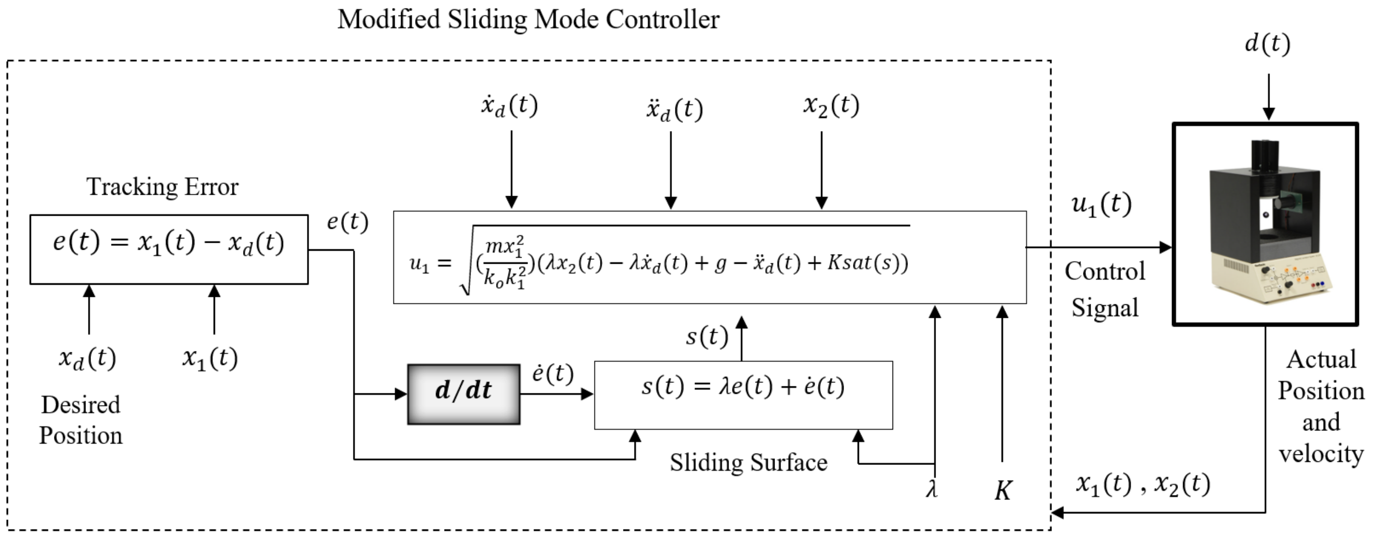

Figure 2. The block diagram of the controlled system using MSMC for the position control of the steel ball of the Maglev model

To design a BSSMC, the backstepping control law is used instead of the equivalent control law in the SMC. To design the backstepping control law, the error $z_2(t)$ between the actual velocity of the ball and the virtual controller is defined as follows [19-22]:

$$z_2(t) = x_2(t) - \alpha(t) \tag{22}$$

where, $\alpha(t)$ is the virtual controller.

Eq. (23) is derived by substituting Eq. (22) into Eq. (11) as follows:

$$\dot{z}_1(t) = z_2(t) + \alpha(t) - \dot{x}_d(t) \tag{23}$$

Using the virtual controller as in Eq. (24), the Eq. (23) is written as follows:

$$\alpha(t) = -c_1 z_1(t) + \dot{x}_d(t) \tag{24}$$

$$\dot{z}_1(t) = -c_1 z_1(t) + z_2(t) \tag{25}$$

where, c_1 a positive design variable.

Taking the time derivative of Eqs. (22) and (24) gives:

$$\dot{z}_2(t) = g - \frac{k_o k_1^2}{m}\frac{u^2(t)}{x_1^2(t)} - \dot{\alpha}(t) \tag{26}$$

$$\dot{\alpha}(t) = -c_1(x_2(t) - \dot{x}_d(t)) + \ddot{x}_d(t) \tag{27}$$

The time derivative of the error $z_2(t)$ can be expressed as follows:

$$\dot{z}_2(t) = -c_2 z_2(t) - z_1(t) \tag{28}$$

where, c_2 is a positive design variable.

The backstepping control law is obtained by substituting Eqs. (9), (22), (24), (27), and (28) in Eq. (26) with some rearrangements as in Eq. (29). Finally, the backstepping sliding mode control law is expressed in Eq. (30). The block diagram of the controlled system using BSSMC for controlling the position of the ball of the Maglev model is shown in Figure 3.

$$u_b = \sqrt{\begin{array}{l}(\frac{m x_1^2}{k_o k_1^2})((c_1 c_2 + 1)x_1(t) + (c_1 + c_2)x_2(t) \\ -(1 + c_1 c_2)x_d(t) - (c_1 + c_2)\dot{x}_d(t) - \ddot{x}_d(t) + g)\end{array}} \tag{29}$$

$$u_2 = \sqrt{\begin{array}{l}(\frac{m x_1^2}{k_o k_1^2})((c_1 c_2 + 1)x_1(t) + (c_1 + c_2)x_2(t) \\ -(1 + c_1 c_2)x_d(t) - (c_1 + c_2)\dot{x}_d(t) - \ddot{x}_d(t) + g + K sat(s))\end{array}} \tag{30}$$

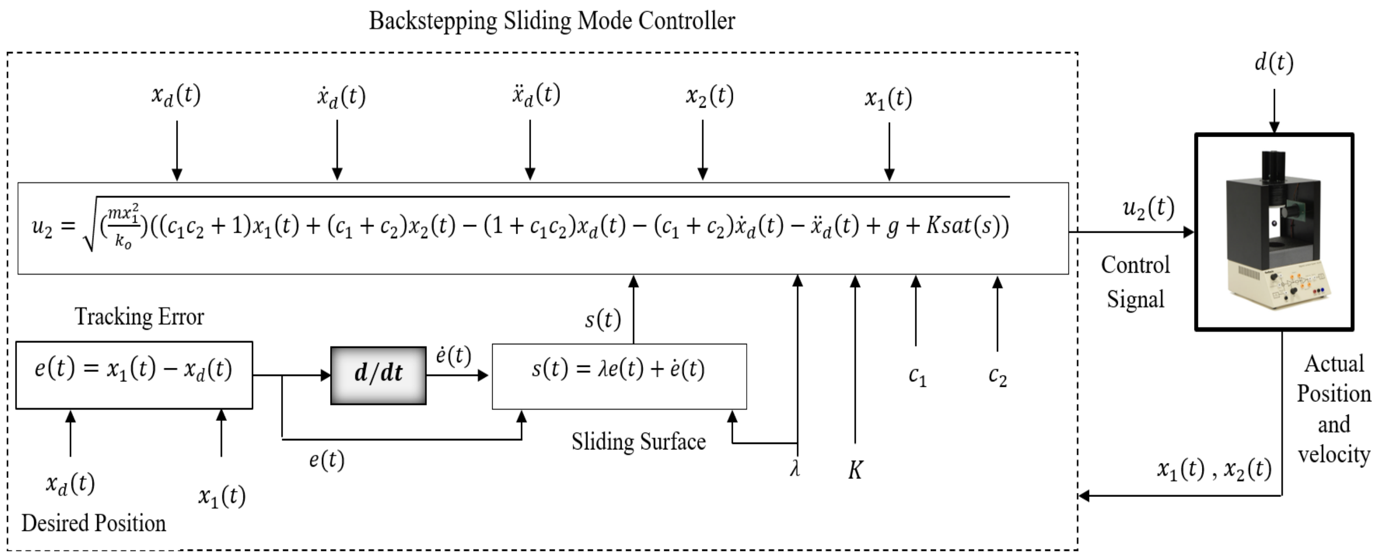

Figure 3. The block diagram of the controlled system using BSSMC for the position control of the steel ball of the Maglev model

4. SIMULATION RESULTS

The designed controllers are simulated and evaluated by numerical simulations conducted in the MATLAB program. The numeric values of Maglev system parameters are presented in Table 1. The parameters of the controllers are chosen using the trial-and-error method and presented in Table 2. The initial values of variables x and $\dot{x}$, which are used to initialize the simulation for the SMC and BSSMC, were chosen as follows: $[x(0), \dot{x}(0)]^T = [0.009, 0]^T$. Two scenarios are used to conduct the simulations, where the results of SMC and BSSMC are compared as follows:

Table 2. The parameter settings of the proposed controllers

Controller	K	Δ	λ	c_1	c_2
MSMC	25	0.5	25	-	-
BSSMC	25	0.5	25	120.25	103.69

4.1 Scenario I

In this scenario, the desired position of the steel ball is fixed at $x_d(t) = 0.01$ m. The Maglev system is subjected to an unknown external force acting as a disturbance. The disturbance is in the form of a pulse signal with a unity magnitude, and the time of the applied pulse is of 5 seconds. The proposed controllers have the ability in forcing the steel ball to follow the desired position as illustrated in Figure 4. Additionally, the settling time of the controlled system using BSSMC is less than that of the controlled system using MSMC. In addition, using the proposed controllers, the steel ball follows the desired position robustly, and the BSSMC is less affected by the perturbation than the MSMC. The velocity of the ball using the proposed controllers is depicted in Figure 5. As seen in this figure, the controlled system dynamic behaviour using the BSSMC is faster than that using the MSMC. The dynamic behaviours of the proposed controllers for the controlling the steel ball position of the Maglev model are presented in Table 3.

The proposed controllers' effectiveness can be deduced from Figure 6, which depicts that the sliding variables reach the sliding manifold after a small period of time. The voltage control efforts of the proposed controllers are smooth, without sharp spikes and within the acceptable range of ± 5 V as

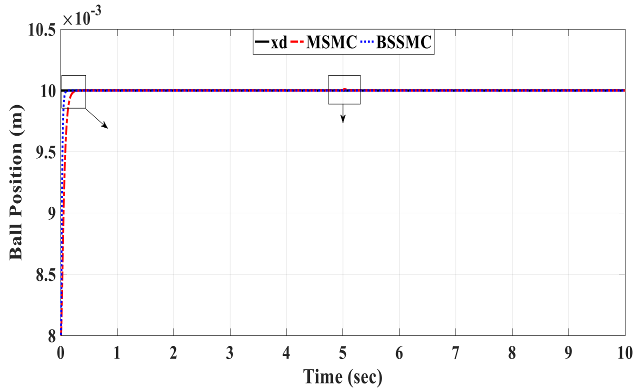

Figure 4. The ball position versus time in scenario I under disturbance

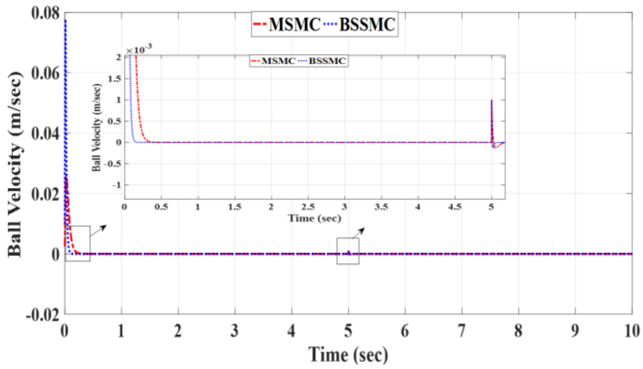

Figure 5. The ball velocity versus time in scenario I under disturbance

Table 3. The output responses of the controlled system for fixed ball position

Controller	Settling Time (T_s) (sec)	Steady-State Error ($E_{s.s}$) (m)	Max. Peak Overshoot Under Disturbance (m)
MSMC	0.5	0	1×10^{-5}
BSSMC	0.2	0	3×10^{-6}
Ref. [14]	1	0	$\pm1\times10^{-4}$

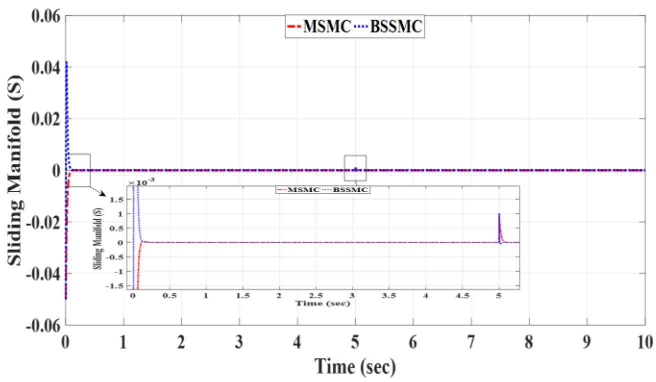

Figure 6. The sliding variable versus time in scenario I under disturbance

demonstrated in Figure 7. Finally, the phase plane between x_1 and x_2 is shown in Figure 8. As illustrated in this figure, the proposed controllers have the ability to force the state to track the desired position ($x_1 = 0.01$ m and $x_2 = 0$ m/sec).

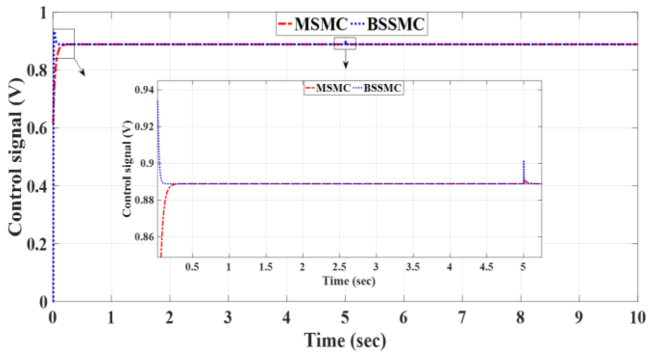

Figure 7. The control signal versus time in scenario I under disturbance

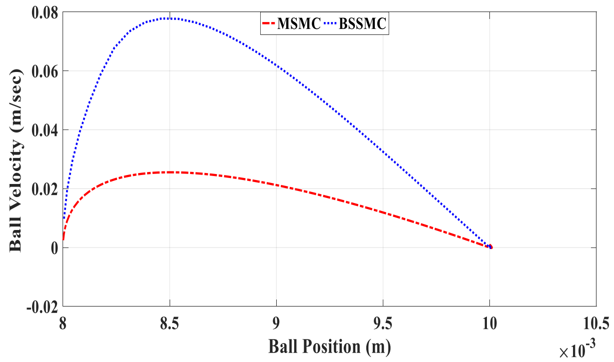

Figure 8. The phase plane versus time in scenario I under disturbance

4.2 Scenario II

The steel ball's desired position in this scenario is variable $x_d(t) = 0.01 + 0.007sin(2\pi t)$ m. The external disturbance exposed to the system is assumed to be the same as in scenario I. The proposed controllers also have the ability to follow the reference variable position, as depicted in Figure 9. According to this figure, the tracking time of the controlled system using BSSMC required to hit and track the desired trajectory is also less than that of the controlled system using MSMC. Moreover, the steel ball robustly tracks the desired variable position, and the BSSMC is less affected by the perturbation than the MSMC. Figure 10 shows the velocity of the ball using the proposed controllers. This figure shows that the controlled system dynamic behaviour using the BSSMC is also faster than that using the MSMC. The proposed controllers' dynamic behaviours for controlling the steel ball position of the Maglev model are illustrated in Table 4.

By using the proposed controllers, the sliding variables converge to the sliding manifold after a small period of time, which demonstrating the effectiveness of these controllers, as depicted in Figure 11. The voltage control efforts produced using the proposed controllers are also smooth, without sharp spikes and within the acceptable range of ± 5 V, as demonstrated in Figure 12. Finally, the phase plane between x_1 and x_2 is depicted in Figure 13. This figure indicates the proposed controllers' effectiveness in driving the state of the system to trace the required sinusoidal position.

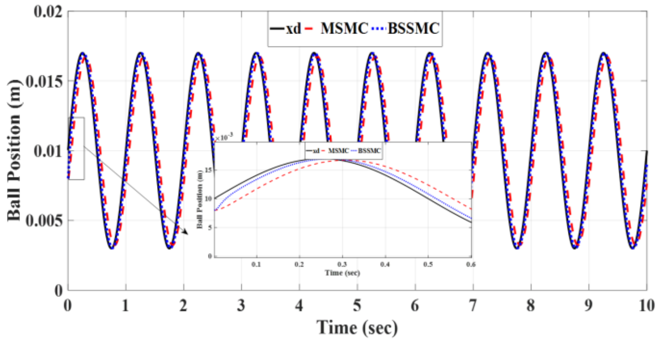

Figure 9. The position of the ball versus time in scenario II under disturbance

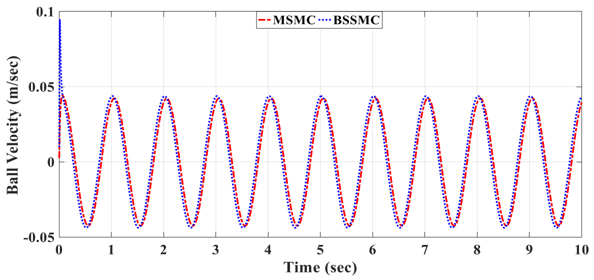

Figure 10. The velocity of the ball versus time in scenario II under disturbance

Table 4. The output responses of the controlled system for variable ball position

Controller	Tracking Time (T_r) (sec)	Steady-State Error ($E_{s.s}$) (m)	Max. Peak Overshoot Under Disturbance (m)
MSMC	0.3	0.055	0
BSSMC	0.2	0.018	0

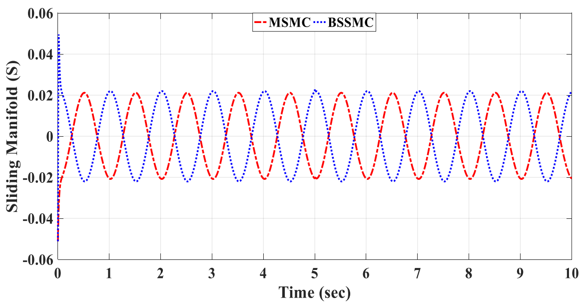

Figure 11. The sliding variable versus time in scenario II under disturbance

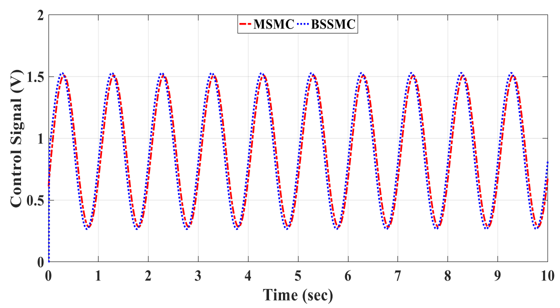

Figure 12. The control signal versus time in scenario II under disturbance

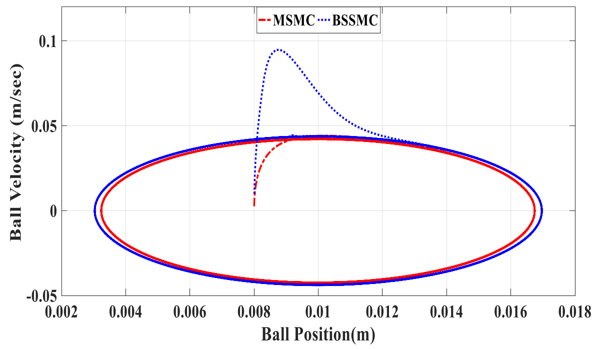

Figure 13. The phase plane versus time in scenario II under disturbance

5. CONCLUSIONS

This work proposes a backstepping sliding mode control strategy for controlling and stabilizing the ball of the Maglev system. The effectiveness of the BSSMC and the MSMC have been examined using computer simulation based on the MATLAB program. A comparative study has been conducted to assess the performance of the BSSMC and the MSMC in conjunction with other controllers. The simulation results show that the performance of the controlled system using the BSSMC is better than that using the MSMC and other controllers in minimizing the settling time for a desired ball position of 0.01 m when the system is exposed to external force disturbance. Moreover, the proposed controllers' effectiveness is validated for sinusoidal input reference. In this case, the controlled system dynamic performance using the BSSMC is also better than that using the MSMC and other controllers in minimizing the tracking time and the steady-state error in the presence of an external disturbance.

For future work, this study can be extended by implementing the backstepping sliding mode control strategy in a real-time environment via LabVIEW programming software or embedded hardware design such as the FPGA [23-25]. Furthermore, another extension of this study is to propose other control techniques for controlling and stabilizing the Maglev system's steel ball to demonstrate their effectiveness and performance in comparison to the proposed BSSMC [26-30].

REFERENCES

[1] Malik, A.S., Ahmad, I., Rahman, A.U., Islam, Y. (2019). Integral backstepping and synergetic control of magnetic levitation system. IEEE Access, 7(1): 173230-173239. https://doi.org/10.1109/ACCESS.2019.2952551

[2] Li, J.H., Li, J., Zhang, G. (2013). A practical robust nonlinear controller for maglev levitation system. Journal of Central South University, 20(11): 2991-3001. https://doi.org/10.1007/s11771-013-1823-1

[3] Šuster, P., Jadlovská, A. (2012). Modeling and control design of magnetic levitation system. In 10th IEEE Jubilee International Symposium on Applied Machine Intelligence and Informatics (SAMI), Herl'any, Slovakia, pp. 295-299. https://doi.org/10.1109/SAMI.2012.6208976

[4] Yaghoubi, H. (2013). The most important maglev

applications. Journal of Engineering, 2013(1): 537986. http://doi.org/10.1155/2013/537986
[5] Jose, J., Mija, S.J. (2020). Particle swarm optimization based fractional order sliding mode controller for magnetic levitation systems. In 2020 IEEE 5th International Conference on Computing Communication and Automation (ICCCA), Greater Noida, India, pp. 73-78. https://doi.org/10.1109/ICCCA49541.2020.9250823
[6] Adil, H.M.M., Ahmed, S., Ahmad, I. (2020). Control of MagLev system using supertwisting and integral backstepping sliding mode algorithm. IEEE Access, 8(1): 51352-51362. https://doi.org/10.1109/ACCESS.2020.2980687
[7] Burakov, M. (2019). Fuzzy PID controller for magnetic levitation system. In Proceedings of 14th International Conference on Electromechanics and Robotics "Zavalishin's Readings" ER (ZR) 2019, Kursk, Russia, pp. 655-663. https://doi.org/10.1007/978-981-13-9267-2_54
[8] Wei, Z., Huang, Z., Zhu, J. (2020). Position control of magnetic levitation ball based on an improved Adagrad algorithm and deep neural network feedforward compensation control. Mathematical Problems in Engineering, 2020: 8935423. https://doi.org/10.1155/2020/8935423
[9] Humaidi, A.J., Badr, H.M., Hameed, A.H. (2018). PSO-based active disturbance rejection control for position control of magnetic levitation system. In 5th International Conference on Control, Decision and Information Technologies (CoDIT), Thessaloniki, Greece, pp. 922-928. https://doi.org/10.1109/CoDIT.2018.8394955
[10] MohammadRidha, T., Kadhim, M.Q. (2022). A barrier function-based variable structure control for maglev system. Journal Européen des Systèmes Automatisés, 55(5): 633-639. https://doi.org/10.18280/jesa.550508
[11] Yadav, S., Verma, S.K., Nagar, S.K. (2016). Optimized PID controller for magnetic levitation system. Ifac-PapersOnLine, 49(1): 778-782. https://doi.org/10.1016/j.ifacol.2016.03.151
[12] Ma'arif, A., Vera, M.A.M., Mahmoud, M.S., Umoh, E., Abougarair, A.J., Rahmadhia, S.N. (2022). Sliding mode control design for magnetic levitation system. Journal of Robotics and Control, 3(6): 848-853. https://doi.org/10.18196/jrc.v3i6.12389
[13] Nayak, A., Subudhi, B. (2016). Discrete backstepping control of magnetic levitation system with a nonlinear state estimator. In 2016 IEEE Annual India Conference (INDICON), Bangalore, India, pp. 1-5. https://doi.org/10.1109/INDICON.2016.7839095
[14] Saikia, A., Baruah, B. (2021). Proposal of sliding mode controller based on backstepping technique for control of magnetic levitation system. International Journal of Engineering and Advanced Technology, 11(2): 1-4. https://doi.org/10.35940/ijeat.A3229.1211221
[15] Waheed, Z.A., Humaidi, A.J (2022). Design of optimal sliding mode control of elbow wearable exoskeleton system based on whale optimization algorithm. Journal Européen des Systèmes Automatisés, 55(4): 459-466. https://doi.org/10.18280/jesa.550404
[16] Hameed, A.H., Al-Dujaili, A.Q., Humaidi, A.J., Hussein, H.A. (2019). Design of terminal sliding position control for electronic throttle valve system: A performance comparative study. International Review of Automatic Control, 12(5): 251-260. https://doi.org/10.15866/ireaco.v12i5.16556
[17] Ajaweed, M.N., Muhssin, M.T., Humaidi, A.J., Abdulrasool, A.H. (2023). Submarine control system using sliding mode controller with optimization algorithm. Indonesian Journal of Electrical Engineering and Computer Science, 29(2): 742-752. https://doi.org/10.11591/ijeecs.v29.i2.pp742-752
[18] Al-hadithy, D., Hammoudi, A.K. (2020). Two- link robot through strong and stable adaptive sliding mode controller. In IEEE 13th International Conference on Developments in eSystems Engineering (DeSE), Liverpool, United Kingdom, pp. 121-127. https://doi.org/10.1109/DeSE51703.2020.9450762
[19] Humaidi, A.J., Hameed, M.R., Hameed, A.H. (2018). Design of block-backstepping controller to ball and arc system based on zero dynamic theory. Journal of Engineering Science and Technology, 13(7): 2084-2105.
[20] Humaidi, A.J., Talaat, E.N., Hameed, M.R., Hameed, A.H. (2019). Design of adaptive observer-based backstepping control of cart-pole pendulum system. In Proceeding of IEEE International Conference on Electrical, Computer and Communication Technologies (ICECCT), Coimbatore, India, pp. 1-5. http://doi.org/10.1109/ICECCT.2019.8869179
[21] Humaidi, A.J., Kadhim, S.K., Gataa, A.S. (2021). Optimal adaptive magnetic suspension control of rotary impeller for artificial heart pump. Cybernetics and Systems, 53(1): 141-167. https://doi.org/10.1080/01969722.2021.2008686
[22] Hamoudi, A.K., Rasheed, L.T. (2023). Design and implementation of adaptive backstepping control for position control of propeller-driven pendulum system. Journal Européen des Systèmes Automatisés, 56(2): 281-289. https://doi.org/10.18280/jesa.560213
[23] Humaidi, A.J., Kadhim, T.M. (2018). Spiking versus traditional neural networks for character recognition on FPGA platform. Journal of Telecommunication, Electronic and Computer Engineering, 10(3): 109-115.
[24] Kasim, M.Q., Hassan, R.F., Humaidi, A.J., Abdulkareem, A.I., Nasser, A.R., Alkhayyat, A. (2021). Control algorithm of five-level asymmetric stacked converter based on Xilinx system generator. In 2021 IEEE 9th Conference on Systems, Process and Control (ICSPC 2021), Malacca, Malaysia, pp. 174-179. https://doi.org/10.1109/ICSPC53359.2021.9689173
[25] Al-Dujaili, A.Q., Falah, A., Humaidi, A.J., Pereira, D.A., Ibraheem, I.K. (2020). Optimal super-twisting sliding mode control design of robot manipulator: Design and comparison study. International Journal of Advanced Robotic Systems, 17(6): 1729881420981524. https://doi.org/10.1177/1729881420981524
[26] Humaidi, A.J., Hasan, S., Al-Jodah, A.A. (2018). Design of second order sliding mode for glucose regulation systems with disturbance. International Journal of Engineering and Technology (UAE), 7(2): 243-247. https://doi.org/10.14419/ijet.v7i2.28.12936
[27] Hassan, M.Y., Humaidi, A.J., Hamza, M.K. (2020). On the design of backstepping controller for Acrobot system based on adaptive observer. International Review of Electrical Engineering, 15(4): 328-335. https://doi.org/10.15866/iree.v15i4.17827
[28] Husain, S.S., Kadhim, M.Q., Al-Obaidi, A.S.M., Hasan, A.F., Humaidi, A.J., Al Husaeni, D.N. (2023). Design of

robust control for vehicle steer-by-wire system. Indonesian Journal of Science and Technology, 8(2): 197-216. https://doi.org/10.17509/ijost.v8i2.54794
[29] Husain, S.S., Rasheed, L.T., Mahmod, R.A., Hamza, E.K., Noaman, N.M., Humaidi, A.J. (2023). Design of RISE control for respiratory system. In 2023 IEEE 8th International Conference on Engineering Technologies and Applied Sciences (ICETAS), Bahrain, pp. 1-5. https://doi.org/10.1109/ICETAS59148.2023.10346523
[30] Husain, S.S., Rasheed, L.T., Mahmod, R.A., Hamza, E.K., Noaman, N.M., Humaidi, A.J. (2023). Design of robust controller for tail-sitter VTOL aircraft. In 2023 IEEE 8th International Conference on Engineering Technologies and Applied Sciences (ICETAS), Bahrain, pp. 1-6. https://doi.org/10.1109/ICETAS59148.2023.10346499

NOMENCLATURE

c_1	dimensionless positive design constant
c_2	dimensionless positive design constant
d	the force disturbance, N
f	the magnetic force
g	acceleration due to gravity, m.s^{-2}
i	the current flowing in the coil, A
i_o	equilibrium value of current, A
K	dimensionless scaler design constant
k_1	control voltage to coil current gain, A.V^{-1}
L	the coil inductance, H
L_o	the increment in inductance due to ball, H
m	mass of the ball, kg
R	the coil resistor, Ω
s	dimensionless sliding surface
sat	the saturation function
u	control input voltage level, V
u_{eq}	the equivalent control law
u_{sw}	the switching control law
u_1	the sliding mode control effort, V
u_2	the backstepping sliding mode control law, V
u_b	The backstepping control law, V
x_d	the desired position, m
x_o	equilibrium value of position, m
x_1	the position of the steel ball, m
x_2	the velocity of the steel ball, m.s^{-1}
z_1	the error between the actual position of the ball and the desired position, m
z_2	the error between the actual velocity of the ball and the virtual controller, m.s^{-1}

Greek symbols

Δ	dimensionless boundary layer thickness
λ	dimensionless scalar design parameter larger than zero
α	the virtual controller, m.s^{-1}